The final publication is available at

https://doi.org/10.1002/cptc.201700049

Additional Information

Multilayer N-doped graphene films as photoelectrodes for H$_2$ evolution

Alejandra Garcia, Josep Albero, and Hermenegildo García*

Abstract: Multilayer N-doped graphene photoelectrodes have been prepared following an easy one-step pyrolytic fabrication method. The N-doped graphene photoelectrodes have demonstrated to work both as semi-transparent electrode and as efficient photoelectrocatalysts for H$_2$ evolution at low bias. N-doped graphene photoelectrodes exhibited constant H$_2$ generation rate of 3.64 µmol/h·cm^2 at 0.2 V under 3443 W/m^2 irradiation for 17 h, reaching an overall quantum yield of 2.6 %. The N-doped graphene photoelectrodes show light intensity dependence as well as photocatalytic activity for H$_2$ evolution in the UV-Vis spectral region. Impedance spectroscopy provides experimental evidence indicating that charge separation within N-doped G increases upon positive bias polarization of the photoelectrode.

Photoelectrocatalysis for the production of H$_2$ from water is one of the most promising approaches for efficient conversion of solar light into chemical energy [1]. Among the various issues that still have to be improved to make this technology closer to application, one of the most important is the nature of the photoelectrodes that should be based on affordable and abundant materials. Another issue is the preparation of durable and efficient photoelectrodes in an easy and scalable manner. Generally, the photoelectrode is constituted by a transparent conductive electrode (TCE) on which a thin film of the semiconductor is deposited. It would be convenient if typically expensive TCEs like fluorine-doped tin oxide (FTO), indium-doped tin oxide (ITO) or aluminium-doped zinc oxide (AZO) are replaced by other amenable and convenient alternatives as layered double hydroxides or silicon, among others [2].

In the present manuscript, it will be described that multilayer defective N-doped graphene (N-G) without the need of TCE ca be a suitable photoelectrode for the generation of H$_2$ at low bias polarization.

Although G has been frequently employed in photocatalysis, most of the reports describe its use in low percentage as additive to increase the photocatalytic efficiency of conventional semiconductors [3]. However, more recently it has been found that graphene oxide (GO) and N-doped Gs have intrinsic photocatalytic activity without the need of inorganic semiconductor [4].

In a series of papers, we have reported that pyrolysis of natural polysaccharides such as alginate and chitosan as nanometric-thick films gives rise to defective single or few-layers

Dr. A. García, Dr. J. Albero and Prof. H. García
Instituto mixto de tecnología química (CSIC-UPV)
Universitat Politècnica de València
Avda. de los Naranjos s/n, E-46022, Valencia, Spain
E-mail: hgarcia@qim.upv.es

Supporting information for this article is given via a link at the end of the document.

G films.[5] When these natural polysaccharide films contain adsorbed Pt, Au, Ag or Cu salts, their pyrolysis leads to films of
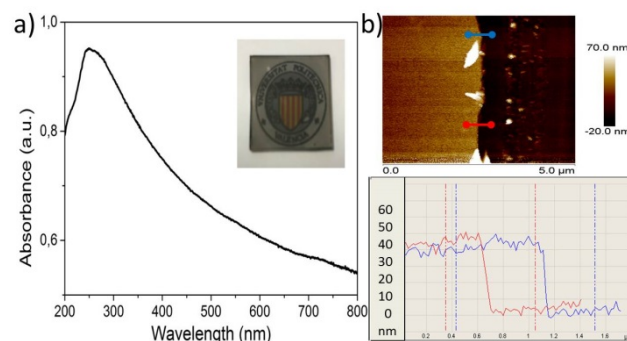

Figure 1. a) UV-Vis absorption spectrum of a N-G photoelectrode (inset shows a digital picture of the University logo through a semitransparent N-G photoelectrode). b) AFM image of a scratched N-G film and the vertical height of two different cross sections.

G having strongly grafted the corresponding metal as nanoplatelets exposing oriented facets.[6] These films of metal nanoplatelets supported on Gs can exhibit high photocatalytic activity for H$_2$ generation from H$_2$O.[7]

Continuing with this line of research and considering that even though much less conductive than ideal defectless G, the samples obtained by pyrolysis of natural polysaccharides still have significant electrical conductivity [5a], it occurred to us that it should be possible to prepare photoelectrodes by pyrolysis of these natural biopolymers on glass or quartz without the need of TCE. In this case the defective G will act both as photocatalyst and as transparent conductive electrode, and in this way a photoelectrode based exclusively on abundant carbon as the only element deposited on electrically insulating material will be developed. The results presented below show that few and multilayer N-G formed by pyrolysis of chitosan films on quartz substrate is able to convert sunlight into H$_2$ with an efficiency of 2.6 % at a low voltage bias of 0.2 V.

N-G photoelectrodes were fabricated by spin coating aqueous solutions of chitosan onto clean quartz substrates and subsequent pyrolysis under Ar atmosphere at 900 °C for 2 h. This one-step preparation method produced semi-transparent N-G films as presented in Figure 1.

The UV-Vis absorption spectrum of a N-G photoelectrode shows the typical continuous band extending from the NIR toward the UV with a maximum peaking at 248 nm, covering completely the visible region of the solar spectrum (Figure 1a), in agreement with previous reports for N-G dispersions [4a]. In spite of this, the N-G films are semi-transparent allowing light to pass through the whole film (see Figure 1 (a) inset). Measurements of the vertical height by AFM of a scratched N-G film have shown that the thickness of the N-G film is approximately 40 nm (Figure 1b). The thickness of the films

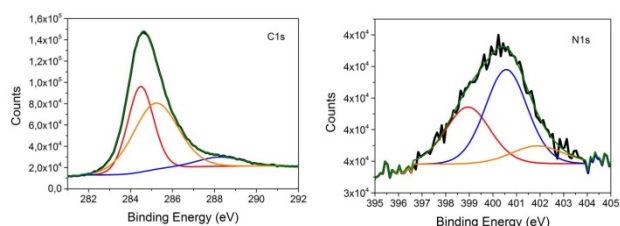controls the electrical conductivity that decreases as the

Figure 2. C1s (left) and N1s (right) XPS spectra of a N-G film.

thickness increases, but also the photoelectrocatalytic activity of the electrode. It should be noted that, as reported, films of few-layers N-G are considerably transparent to the visible radiation [5a] and, therefore, having much less photocatalytic response. A compromise can be reached by increasing film thickness. Adequate thickness (about 40 nm) contributes to obtain proper light absorption and a film resistivity of 1.5 kΩ□ obtained from a set of four-tips conductivity measurements.

The C1s and N1s XPS peaks and their best deconvolution to individual components are presented in Figure 2. This analysis indicates that the C1s peak fits well as being a combination of three main types of C atoms corresponding to graphenic sp^2 carbons (284.5 eV), carbons bonded to nitrogen (285.5 eV) and C=O (288.4 eV). The origin of the oxygen and nitrogen atoms present in these defective graphenes (~ 15% and 2 % for O and N, respectively) is the chitosan precursor that is a polysaccharide of glucosamine. Similarly, the deconvolution of the N1s peak revealed three components that can be attributed to quaternary N (398.9 eV), pyridinic N (400.5 eV) and some N-oxides at 402.1 eV.

It should be commented that the N content in the N-G films could be varied below 7 % by controlling the pyrolysis conditions, mainly the final temperature and the time, as it has been reported before [8].

Linear-sweep voltammograms (LSV) were carried out with N-G photoelectrodes at 10 mV·s^{-1}, using aqueous Na$_2$S/Na$_2$SO$_3$ solutions as electrolyte, in dark and under illumination by a 300 W Xe lamp in order to evaluate the possible photoresponse of the N-G electrodes. The results are presented in Figure 3.
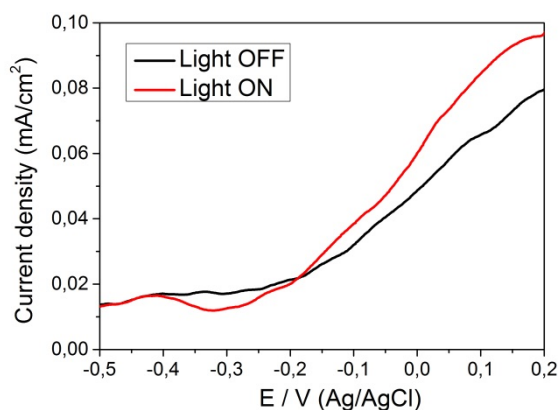

Figure 3. LSV at 10 mV·s^{-1} of a N-G photoelectrode in Na$_2$S/Na$_2$SO$_3$ electrolyte in dark (red) and under 3443 W/m^2 illumination (black). A Pt wire was used as counter electrode and Ag/AgCl as reference electrode.

As can be seen in Figure 3, the current density in N-G photoelectrodes measured at negative potentials up to -0.2 V vs. Ag/AgCl presented no differences between light and dark. However, starting from -0.2 V towards positive potentials, the current density upon light illumination was consistently higher than in the dark, increasing the difference between dark and light current along the value of the positive bias potential applied. A maximum current density of 98 μA/cm^2 under light irradiation was reached at +0.2 V, while under dark conditions the current density was 80 μA/cm^2 at the same potential (see Figure 3). The increase in current density upon light illumination indicates that the N-G photoelectrodes are capable to photogenerate charges and this could be reflected in an increased efficiency of the electrochemical reaction.

This higher efficiency of the photoelectrocatalytic process was confirmed by measuring the hydrogen production from N-G electrode in the dark and under illumination. The results are presented in Figure 4.

Constant hydrogen production rates during 17 h under light illumination of 3.64, 1.53 and 1.38 μmol/h·cm^2 were measured for 0.2 V, open circuit and – 0.2 V applied bias, respectively. The trend of H$_2$ production rates as a function of the bias potential in which H$_2$ generation is higher at positive than at negative bias indicates that the N-G photoelectrode is working as photoanode, rather than photocathode. The linear relationship between the H$_2$ production and time indicates that the N-G electrode is stable with respect to its photoelectrocatalytic ability during the experiment for 17 h. The hydrogen production in the dark was about 1.2 μmol/h·cm^2 at 0.2 V. Thus,
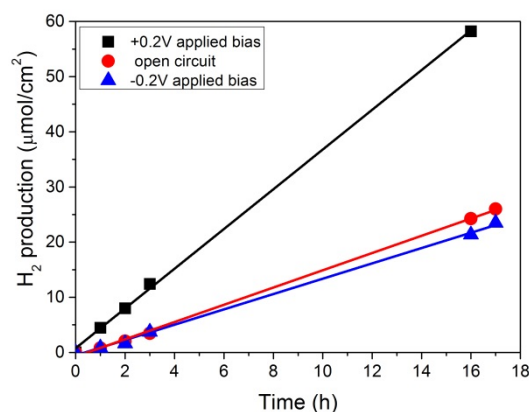

Figure 4. Hydrogen evolution rate obtained from N-G electrode at different applied bias under 3443 W/m^2 irradiation from a Xe lamp. Aqueous solutions of Na$_2$S/Na$_2$SO$_3$ were used as electrolyte, a Pt wire as counter electrode and Ag/AgCl as reference.

light produced 3-fold increase in the hydrogen production rate, reaching a solar-to-hydrogen efficiency (STH)[9] of 0.16% while applied-bias-compensated solar-to-hydrogen efficiency (AB-STH)[9] was of 1.8 %.

In order to fully address electrode stability as a function of the applied bias on the photocatalytic H$_2$ production with N-G photoelectrodes, chronoamperometric (CA) tests at 0.2 V and -0.2 V vs. Ag/AgCl under light irradiation with the Xe lamp were carried out. Figure 5 presents the current density time evolution upon light irradiation at the two different potentials. It

was observed there, that the current density decreases from about 100 $\mu A/cm^2$ to 40 $\mu A/cm^2$ in 15 h under 0.2 V bias, although it seems that it has become stationary beyond 10 h. In contrast, at -0.2 V bias, the current intensity of N-G electrode suddenly decreases from an initial value of 65 $\mu A/cm^2$ in the first seconds, then becomes stable for about 6 h at a value about 30 $\mu A/cm^2$ and finally decreases until it is very beyond 13 h. Worth noting is that a large percentage of the current indicated in Figure 5 is spurious and wasted as recombination losses, internal resistance and heat. Thus, knowing the steady H_2 generation rate shown in Figure 4, at a bias potential of 0.2 V about 28 % of the stationary 40 $\mu A/cm^2$ current is converted to H_2 (see Faradaic efficiency in Equation 2 of experimental section). When the bias potential is -0.2 V all the consumed current is lost, since the photoelectrocatalytic H_2 production coincides with the photocatalytic H_2 production and no additional H_2 is generated (see Figure 4).

Photoelectrocatalytic tests were carried out at different light intensities in order to confirm the photocatalytic activity in N-G photoelectrodes. Neutral density filters with 39 and 63 % transmittance over the whole spectral range were used to filter the 3443 W/m^2 output of our lamp. The results of the influence of light intensity on the photocatalytic H_2 generation are presented in Figure 6 (top). As can be observed, decreasing the light intensity results in a notable decrease in the H_2 evolution indicating that photogenerated charges contribute in a significant extent to the photoelectrocatalytic activity of the N-G electrode.
It is, however, worth noticing that the decrease in H_2 evolution does not follow a linear relationship with the decrease in light intensity. This is probably an artifact due to the spectral response of the neutral density filter utilized in this study that as can be observed in Figure SI1 in Supplementary Information has a preferential filter effect in the UV region. Thus, as it can be seen in this Figure SI1, although the transmittance in the visible and NIR regions is practically constant, the transmittance in the UV region is drastically reduced.
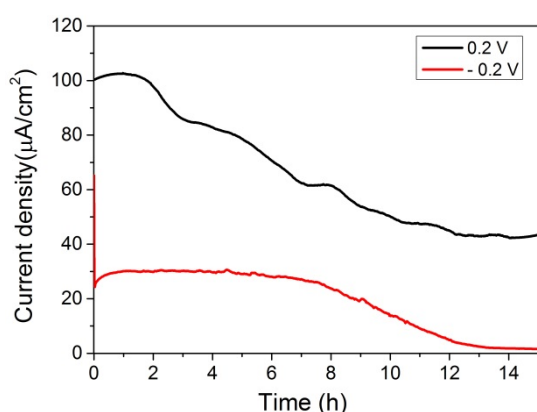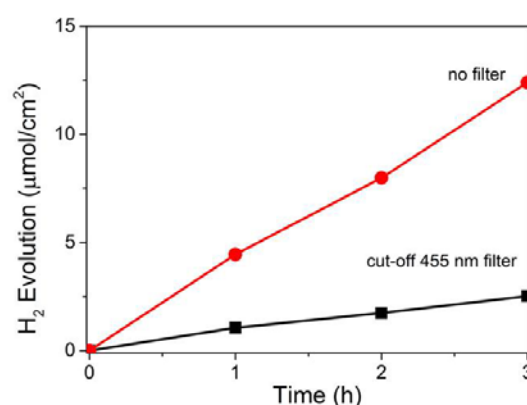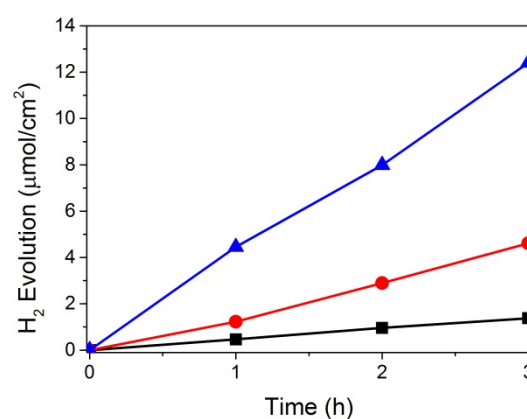

Figure 6. H_2 production under different light intensities 3443 (blue), 2169 (red) and 1343 (black) mW/cm^2 (top) and using a cut-off filter at 455 nm under 2327 mW/cm^2 (bottom) using N-G photoelectrodes at 0.2 V vs. Ag/AgCl. Reaction conditions: Aqueous solutions of Na_2S/Na_2SO_3 were used as electrolyte, a Pt wire as counter electrode and Ag/AgCl as reference.

Therefore, the higher than expected decrease in H_2 production with respect to the light intensity decrease when these filters were used is due not only to the decrease in light power, but also to the preferential cut-off of the UV region caused by these neutral filters. In fact, when a cut-off filter at 455 nm was used in order to elucidate the photoresponse of the N-G electrodes in the visible region a substantial decrease in the amount of H_2 evolution was observed as seen in Figure 6 (bottom). As it can be observed there, although the N-G electrodes are still active upon irradiation in the visible region for wavelengths larger than 455 nm, the major photoresponse is observed in the UV region below 455 nm, in good agreement with the UV-Vis absorption spectra of the N-G electrode (Figure 1).

Electrochemical impedance spectroscopy (EIS) was used to study the charge transfer processes taking place at the N-G electrodes in the photoelectrocatalytic H_2 evolution reaction. The Nyquist plot under illumination at different bias potentials is presented in Figure 7.

Figure 5. CA test of N-G photoelectrodes at 0.2 V (black) and -0.2 V (red) vs. Ag/AgCl in Na_2S/Na_2SO_3 electrolyte. A Pt wire was used as counter electrode and Ag/AgCl as reference electrode.
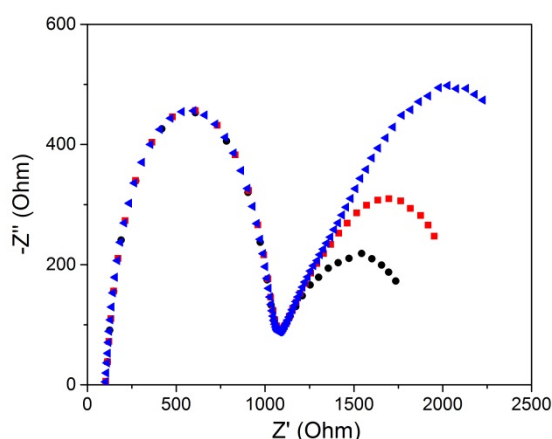
Figure 7. Nyquist plots for N-G photoelectrode at 0.2 V (black), open circuit (red) and -0.2 V(blue) bias under illumination.

Two semicircles were observed in EIS as reported before in similar photoelectrodes.[10] Bisquert et al. proposed that each semicircle represents a capacitive resistive (RC) element due to charge transfer processes in the photoelectrode and between the photoelectrode/electrolyte interface. [10b] Accordingly, the first semicircle in the high frequency range was attributed to the impedance given by charge transfer at the electrode and the second semicircle at low frequency range has been related to the charge transfer impedance of electron recombination reactions at the semiconductor/electrolyte interface. It has been suggested that smaller arc radius in the Nyquist plot implies more efficient charge separation of electron-hole pairs and faster interfacial charge transfer processes [11].

In the present case, the high frequency semicircle did not change with the applied bias, indicating that the charge transfer processes in the photoelectrode do not depend on the applied potential. However, the second semicircle arc radius increased at applied negative bias, suggesting an increase of the resistance in the N-G photoelectrode/electrolyte interface at negative bias, probably due to a more favorable charge recombination as the negative bias polarization increases. The semicircles obtained in the Nyquist plot (Figure 7) have been fitted with a R-C model equivalent circuit similar to previous EIS studies of semiconductor based photoelectrodes (equivalent circuit and modeled R-C values are listed in Figure SI2 and Table SI1, respectively, in Supplementary Information) [12].

It is well known that in photoelectrochemical reactions the efficiency of charge separation of photogenerated charges increases with the external bias.[13] Therefore, the data obtained indicate that the photogenerated charges in the N-G photoelectrodes are more efficiently separated at positive 0.2 V potential, where the electrode acts as anode, while negative -0.2 V potential enhanced charge recombination and, as consequence, H_2 production is decreased. Scheme 1 illustrates the difference between these two scenarios.
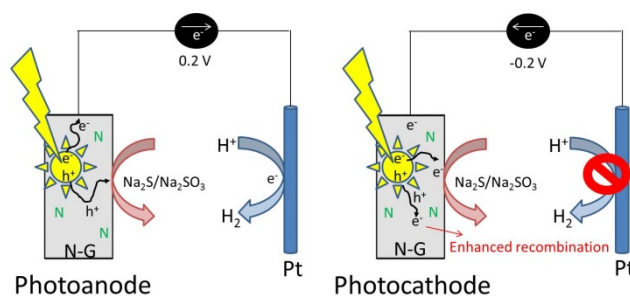
Scheme 1. N-G photoelectrode working under light illumination and positive 0.2 V applied bias (left) and N-g photoelectrode working under negative -0.2V applied bias under illumination.

In conclusion, in the present work it has been shown the preparation of photoelectrodes based exclusively on N-doped G by pyrolysis of chitosan on arbitrary non-conductive supports, such as quartz. In these photoelectrodes, N-doped G acts as semiconductor and conductive electrode. The resulting electrode exhibits photoelectrocatalytic activity for H_2 generation at low potential bias, showing constant H_2 production 17 h. Chronoamperometry shows, however, a decrease of the initial current of about 50% for 10 h irradiation. Most of the photoresponse of N-G derives from the UV region, although some residual activity in the visible light has been observed. The present findings opens the way for photoelectrodes based exclusively on doped Gs in which this material can play the role of current collector and photocatalyst. Improvement in the efficiency and stability of these graphene-based photoelectrodes can avoid the need in the composition of photoelectrodes of the use of critical and precious metals.

Experimental Section

N-G photoelectrodes were prepared by pyrolysis of chitosan films as reported before [5a]. In brief, low molecular weight chitosan (Sigma Aldrich) aqueous solution containing acetic acid was spin coated on previously cleaned quartz substrates of 3 cm². The chitosan films were dried at 70 °C and heated at 5 °C/min up to 900 °C, maintaining this temperature for 2 h under Ar atmosphere. The system was allowed to cool down under continuous Ar flux.

Photoelectrochemical experiments were carried out in a quartz cylindrical three-electrode cell on a Versastat electrochemical workstation with N-G photoelectrode as the working electrode, a platinum foil as the counter electrode and Ag/AgCl (saturated KCl) as the reference electrode. The working electrode was irradiated using a UV-Vis 300 W Xe lamp as light source through an optical fiber that irradiates the photoelectrode from the front. Cyclic voltammetric curves and chronoamperometric curves were measured in 0.2 M Na_2S and 0.3 M Na_2SO_3 as electrolyte, previously purged with argon gas. Electrochemical impedance spectroscopy was carried out with an Amel electrochemical workstation between 10^{-1} - 10^6 Hz of frequency.

The STH and AB-STH were calculated from Equation 1 and 2, respectively.

$$STH = \frac{r_{H2} \times \Delta G}{P_{Sun} \times S}$$

Equation 1,

where, r_{H2} is the hydrogen production ($4.86 \cdot 10^{-8}$ mol/s), ΔG is the gain in Gibbs energy (33.4 KJ/mol considering the presence of S^{2-} as sacrificial electron donor, H_2S into H_2 and S), P_{Sun} is the energy flux (3443 W/m^2) and S the area (3 cm^2).

$$AB - STH = \frac{|j| \times n_F \times (V_{Th} - V_{bias})}{P_{sun}}$$ Equation 2,

Where, j is photocurrent density ($60 \cdot 10^{-3}$ A/cm^2), η_F is the faradaic efficiency (12.19 µA/cm^2 consumed in forming H2 divided by 43 12.19 µA/cm^2 of steady current after 12 h= 0.28), $(V_{Th} - V_{Bias})$ = 0.4 and P_{Sun} is the energy flux (0.3443 W/cm^2).

Acknowledgements

[1]   aG. G. Bessegato, T. T. Guaraldo, J. F. de Brito, M. F. Brugnera, M. V. B. Zanoni, *Electrocatalysis* **2015**, *6*, 415-441; bS. Perathoner, G. Centi, D. Su, *ChemSusChem* **2016**, *9*, 345-357; cC. Ding, J. Shi, Z. Wang, C. Li, *ACS Catalysis* **2017**, *7*, 675-688.

[2]   aM. Zhuang, X. Ou, Y. Dou, L. Zhang, Q. Zhang, R. Wu, Y. Ding, M. Shao, Z. Luo, *Nano Letters* **2016**, *16*, 4691-4698; bZ. Xia, X. Zhou, J. Li, Y. Qu, *Science Bulletin* **2015**, *60*, 1395-1402; cY. Zhao, X. Jia, G. I. N. Waterhouse, L.-Z. Wu, C.-H. Tung, D. O'Hare, T. Zhang, *Advanced Energy Materials* **2016**, *6*, n/a-n/a.

[3]   aX. Zhang, J. Wang, W. Hu, K. Zhang, B. Sun, G. Tian, B. Jiang, K. Pan, W. Zhou, *ChemCatChem* **2016**, *8*, 3240-3246; bZ. Pan, T.

Hisatomi, Q. Wang, S. Chen, A. Iwase, M. Nakabayashi, N. Shibata, T. Takata, M. Katayama, T. Minegishi, A. Kudo, K. Domen, *Advanced Functional Materials* **2016**, *26*, 7011-7019; cW. Tu, Y. Zhou, Z. Zou, *Advanced Functional Materials* **2013**, *23*, 4996-5008.

[4]   aC. Lavorato, A. Primo, R. Molinari, H. Garcia, *Chemistry – A European Journal* **2014**, *20*, 187-194; bT.-F. Yeh, J. Cihlář, C.-Y. Chang, C. Cheng, H. Teng, *Materials Today* **2013**, *16*, 78-84.

[5]   aA. Primo, P. Atienzar, E. Sanchez, J. M. Delgado, H. Garcia, *Chemical Communications* **2012**, *48*, 9254-9256; bA. Primo, E. Sanchez, J. M. Delgado, H. Garcia, *Carbon* **2014**, *68*, 777-783.

[6]   aI. Esteve-Adell, N. Bakker, A. Primo, E. Hensen, H. Garcia, *Acs Applied Materials & Interfaces* **2016**, *8*, 33690-33696; bS. Frindy, A. El Kadib, M. Lahcini, A. Primo, H. Garcia, *Acs Catalysis* **2016**, *6*, 3863-3869; cA. Primo, I. Esteve-Adell, J. F. Blandez, A. Dhakshinamoorthy, M. Alvaro, N. Candu, S. M. Coman, V. I. Parvulescu, H. Garcia, *Nature Communications* **2015**, *6*; dA. Primo, I. Esteve-Adell, S. N. Coman, N. Candu, V. I. Parvulescu, H. Garcia, *Angewandte Chemie-International Edition* **2016**, *55*, 607-612.

[7]   aD. Mateo, I. Esteve-Adell, J. Albero, A. Primo, H. Garcia, *Applied Catalysis B-Environmental* **2017**, *201*, 582-590; bD. Mateo, I. Esteve-Adell, J. Albero, J. F. S. Royo, A. Primo, H. Garcia, *Nature Communications* **2016**, *7*.

[8]   H. G. Baldoví, F. Albarracín, M. Álvaro, B. Ferrer, H. García, *ChemPhysChem* **2015**, *16*, 2094-2098.

[9]   T. Hisatomi, J. Kubota, K. Domen, *Chemical Society Reviews* **2014**, *43*, 7520-7535.

[10]   aA. P. Upadhyay, D. K. Behara, G. P. Sharma, M. Gyanprakash, R. G. S. Pala, S. Sivakumar, *ACS Sustainable Chemistry & Engineering* **2016**, *4*, 4511-4520; bB. Klahr, S. Gimenez, F. Fabregat-Santiago, T. Hamann, J. Bisquert, *Journal of the American Chemical Society* **2012**, *134*, 4294-4302.

[11]   Q. Li, M. Zheng, M. Zhong, L. Ma, F. Wang, L. Ma, W. Shen, *Scientific Reports* **2016**, *6*, 29738.

[12]   Y. Zhou, Q. Zhang, Y. Lin, E. Antonova, W. Bensch, G. R. Patzke, *Science China Chemistry* **2013**, *56*, 435-442.

[13]   H. Liu, S. Cheng, M. Wu, H. Wu, J. Zhang, W. Li, C. Cao, *The Journal of Physical Chemistry A* **2000**, *104*, 7016-7020.

Layout 1:

COMMUNICATION

Multilayer N-doped graphene photoanodes have been prepared through one-step preparation method. The as-prepared photoanodes exhibit photocatalytic activity in the UV-Vis region for H_2 evolution reaction.
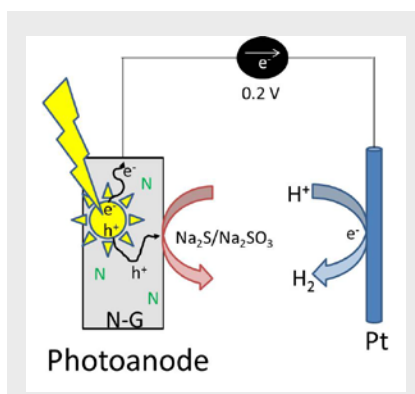
Alejandra García, Josep Albero and Hermenegildo García*

Page No. – Page No.

Multilayer N-doped graphene films as photoelectrodes for photoelectrocatalytic H_2 evolution